

The Preservation Tradeoff: A Thermodynamic Bound in the Diminishing-Returns Regime

Amadeus Brandes
 Independent Researcher, Germany
 brandesamadeus@gmail.com

Abstract

Thermodynamic systems that preserve information against thermal fluctuations face a tradeoff distinct from transmission (Shannon) or erasure (Landauer). We establish a feasibility condition for this preservation problem within a broad class of systems exhibiting diminishing returns in error suppression. By defining the preservation stiffness S_κ , a response function analogous to magnetic susceptibility, we derive an optimality condition linking S_κ to the resource odds. This identity provides a substrate-agnostic diagnostic: deviations reveal thermodynamic inefficiency or operation outside the smooth reliability regime. For systems in the diminishing-returns regime—a class we argue is typical of physically realistic error-correction—the optimal maintenance allocation is bounded above by 50%; for the physically significant subclass exhibiting smooth saturation, it is further constrained to a 30–50% band. We derive this regime from two independent physical principles—Shannon’s channel capacity and Landauer’s erasure bound—whose convergence on the same functional form constitutes our central theoretical contribution. We validate this framework against kinetic proofreading data in *E. coli* and protocol overhead in TCP/IP networks, and specify conditions under which the prediction is falsifiable.

1 Introduction

The thermodynamics of information is grounded in two well-defined limits. Shannon’s noisy channel coding theorem bounds the rate of infor-

mation transmission by the channel capacity C Shannon [1948]. Landauer’s principle bounds the cost of information erasure by $k_B T \ln 2$ Landauer [1961].

However, physical systems often face a third distinct challenge: *preservation*. From DNA repair mechanisms to error-correcting memory in computation, systems must actively suppress entropy generation to maintain a target macrostate over time. Unlike transmission (moving bits) or erasure (resetting bits), preservation involves the continuous maintenance of state fidelity against a thermal bath. While processes like kinetic proofreading occur during the transmission of genetic information, we treat the excess dissipation driving the discrimination step specifically as the maintenance overhead required to preserve fidelity.

This problem has been treated in specific contexts—reliability engineering, kinetic proofreading Hopfield [1974], and finite-blocklength coding theory Gallager [1965], Polyanskiy et al. [2010]—but always in model-specific, dimensional terms. Unlike prior work analyzing specific mechanisms, we derive a substrate-agnostic constraint that links maintenance overhead directly to a response function S_κ , yielding a bound comparable in form to capacity or Landauer’s limit.

Related perspectives include stochastic thermodynamics of information processing Seifert [2012], Parrondo et al. [2015] and the finite-blocklength approach to channel coding Polyanskiy et al. [2010], which bound error probability as a function of redundancy. Our contribution is to recast the preservation problem in the lan-

guage of fluctuation-response theory, identifying the stiffness \mathcal{S}_κ as the natural control variable.

We show that for systems operating in the diminishing-returns regime—where each additional unit of maintenance investment yields progressively smaller gains in reliability—the optimal maintenance fraction κ^* is confined to a narrow interior band, typically between 0.30 and 0.50 of total system capacity. Crucially, we derive this regime from two independent physical routes: information-theoretic constraints on error exponents and thermodynamic constraints on dissipation. The convergence of these routes on the same functional form (Section 3) constitutes the paper’s central theoretical contribution. The inclusion of a non-biochemical system (TCP/IP) alongside molecular proofreading is deliberate: it probes whether the preservation band reflects thermodynamic dissipation specifically or the generic allocation structure $(1 - \kappa)\Delta R(\kappa)$ under diminishing returns, with ΔR denoting reliability gain above any nonzero baseline.

2 Formalism: The Preservation Stiffness

Consider a system with total resource capacity normalized to unity. This capacity is partitioned into payload $(1 - \kappa)$ and maintenance κ . The system’s effective throughput is defined as

$$T_{\text{eff}}(\kappa) = (1 - \kappa)R(\kappa), \quad (1)$$

where $R(\kappa)$ is the reliability (probability of correctness) as a function of maintenance investment.

To establish the generality of this framework, we map the variables to their physical counterparts in Table 1. This mapping reveals that preservation is a universal thermodynamic class, distinct from the specific substrate (biological, electronic, or algorithmic).

To characterize the response of the system to maintenance injection, we define the *preservation stiffness*

$$\mathcal{S}_\kappa \equiv \frac{R(\kappa)}{\kappa R'(\kappa)} = \left(\frac{\partial \ln R}{\partial \ln \kappa} \right)^{-1}. \quad (2)$$

This quantity is the inverse of the elasticity of reliability. In thermodynamic terms, it measures the stiffness of the error-suppression mechanism. A low \mathcal{S}_κ implies that reliability is highly sensitive to marginal maintenance investment (soft mode), while a high \mathcal{S}_κ implies saturation (stiff mode).

Assume R is differentiable on $(0, 1)$ and that the optimum occurs at an interior point $\kappa^* \in (0, 1)$; corner optima ($\kappa^* \in \{0, 1\}$) correspond to degenerate regimes (no maintenance or no payload) and are excluded from the stiffness condition. Maximizing Eq. (1) yields the first-order condition $-R(\kappa^*) + (1 - \kappa^*)R'(\kappa^*) = 0$. Rearranging and substituting the definition of \mathcal{S}_κ , we obtain the **Stiffness-Odds Identity**:

$$\mathcal{S}_\kappa(\kappa^*) = \frac{1 - \kappa^*}{\kappa^*} \quad (3)$$

This identity is the central result of this paper. All subsequent bounds on κ^* follow from Eq. (3) combined with constraints on \mathcal{S}_κ . The identity converts the problem of predicting optimal allocation into the problem of bounding a single response function. The right-hand side is the *resource odds*—the ratio of payload capacity to maintenance capacity. At optimal efficiency, the system’s stiffness must match this resource leverage.

This identity provides a diagnostic for thermodynamic efficiency. If $\mathcal{S}_\kappa > (1 - \kappa)/\kappa$, the system is in a *stiff mode*—over-investing in saturated maintenance and wasting payload capacity. If $\mathcal{S}_\kappa < (1 - \kappa)/\kappa$, the system is in a *soft mode*—under-investing despite high responsiveness, resulting in suboptimal throughput due to excessive error rates. Equilibrium occurs when stiffness matches resource odds.

3 Physical Derivation of the Diminishing-Returns Regime

The critical physical question is the functional form of $R(\kappa)$. We now show that the exponential-saturation form $R(\kappa) = 1 - e^{-g(\kappa)}$ with concave g emerges from two independent physical principles. This dual derivation—

Table 1: The Preservation Rosetta Stone: Mapping thermodynamic variables across substrates. The stiffness \mathcal{S}_κ serves as the universal response function linking these domains.

Variable	Symbol	Thermodynamics	Protocol / Biology
Capacity	1	Free Energy (F)	Bandwidth / GTP Budget
Maintenance	κ	Dissipated Work (W_{diss})	Overhead / Proofreading
Reliability	$R(\kappa)$	State Fidelity	Goodput / Accuracy
Efficiency	a	Coupling ($\Delta E/k_B T$)	Signal-to-Noise Ratio
Response	\mathcal{S}_κ	Stiffness (Inverse χ)	Saturation metric

from information theory and thermodynamics—constitutes the paper’s main theoretical contribution: the same functional constraint arises from entirely different physical considerations.

3.1 Information-Theoretic Route

Consider a system that must maintain state fidelity over a noisy channel with finite capacity C . The fundamental constraint is Shannon’s noisy channel coding theorem: reliable communication requires coding rate $r < C$ Shannon [1948].

For finite blocklength n , Gallager’s error exponent bounds give the probability of decoding error Gallager [1965]:

$$P_{\text{error}} \sim \exp(-n \cdot E(r)), \quad (4)$$

where $E(r)$ is the reliability function (error exponent) of the channel, which depends on the coding rate r and satisfies $E(r) > 0$ for $r < C$ and $E(C) = 0$.

Now interpret n as the redundancy devoted to error protection, proportional to maintenance investment κ . Writing $n = \beta\kappa$ for some constant β (the redundancy per unit maintenance), we have:

$$\varepsilon(\kappa) = 1 - R(\kappa) \sim \exp(-\beta\kappa \cdot E(r)). \quad (5)$$

Key property: The reliability function $E(r)$ is concave in the coding rate r and satisfies $E(r) \rightarrow 0$ as $r \rightarrow C$. Finite-blocklength analysis Polyanskiy et al. [2010] refines this picture: for systems operating below capacity, the achievable error probability decays at most exponentially in blocklength, with rate determined by $E(r)$.

Inverting, we obtain $R(\kappa) = 1 - \exp(-g(\kappa))$ where $g(\kappa) = \beta\kappa \cdot E(r)$. For a fixed operating rate $r < C$, $E(r)$ is a positive constant and $g(\kappa)$ is *linear* (hence concave) in κ . Nonlinear concave g arises when the effective exponent per unit redundancy decreases with κ due to coding/decoding constraints, feedback, or other saturation mechanisms; we capture this general behavior with the concave g assumption in Definition 1.

Key constraint from information theory: The rate parameter $a = g'(0)$ depends on both the channel (through $E(r)$) and the coding efficiency (through β). For any fixed channel and coding scheme operating below capacity, a is finite and positive. The essential point is not a specific bound on a , but rather that the exponential-saturation form $R(\kappa) = 1 - e^{-g(\kappa)}$ with concave g emerges from the structure of channel coding.

3.2 Thermodynamic Route

Consider the same preservation problem from the perspective of thermodynamic dissipation. Maintaining reliability $1 - \varepsilon$ against thermal fluctuations requires exporting entropy from the system. As recently derived for molecular templating networks, maintaining such non-equilibrium low-entropy states imposes a fundamental free-energy cost Qureshi et al. [2025].

By Landauer’s principle Landauer [1961], erasing one bit of information requires dissipation of

at least $k_B T \ln 2$. Error correction fundamentally involves acquiring information about the error state and erasing it—each corrected error requires entropy export.

The Crooks fluctuation theorem provides a more general constraint Crooks [1999]. For a system driven between states, the ratio of forward to reverse transition probabilities satisfies:

$$\frac{P_F}{P_R} = \exp\left(\frac{W - \Delta F}{k_B T}\right), \quad (6)$$

where W is the work performed and ΔF is the free energy difference. For error correction, the “forward” process is successful maintenance (keeping the correct state) while the “reverse” is error occurrence.

Maintaining error probability ε against thermal noise requires suppressing incorrect transitions. From Eq. (6), the ratio of correct to incorrect state occupancy scales as $\exp(\beta W)$ where $\beta = 1/(k_B T)$ and W is the dissipation devoted to error suppression. Thus:

$$\varepsilon \sim \exp(-\beta W). \quad (7)$$

If maintenance investment κ translates to dissipation $W = \gamma \kappa$ (where γ is the available free energy per unit maintenance), we obtain:

$$R(\kappa) = 1 - \exp(-\beta \gamma \kappa). \quad (8)$$

More generally, the second law constrains the efficiency of any error-correction process. Stochastic thermodynamics Seifert [2012], Parondo et al. [2015] establishes that the information gained about a system’s state is bounded by the dissipation:

$$I_{\text{gained}} \leq \frac{W_{\text{diss}}}{k_B T \ln 2}. \quad (9)$$

Since error correction requires gaining information about errors, the rate of error suppression is bounded by available dissipation.

Key constraint from thermodynamics: The rate parameter $a = g'(0) = \beta \gamma$ is bounded above by the available free energy per unit maintenance:

$$a \leq \frac{\Delta G_{\text{available}}}{k_B T \cdot (\text{maintenance unit})}. \quad (10)$$

3.3 Convergence: The Efficiency Frontier as an Attractor

The information-theoretic and thermodynamic routes converge on the same functional form:

$$R(\kappa) = 1 - \exp(-g(\kappa)), \quad g \text{ concave, } g(0) = 0, g' > 0. \quad (11)$$

This convergence is not coincidental. **Error correction is entropy export.** Shannon’s channel capacity and Landauer’s erasure bound are manifestations of the same underlying constraint: the rate at which a system can reduce uncertainty (whether interpreted as decoding errors or thermodynamic fluctuations) is bounded by its information-processing or dissipation capacity.

The rate parameter $a = g'(0)$ is not a universal constant but a system-specific figure of merit representing the coupling efficiency between maintenance resources and error suppression. It admits dual interpretations:

- **Information theory:** Channel capacity per unit redundancy
- **Thermodynamics:** Available free energy per unit maintenance (in units of $k_B T$)

While a can theoretically take any positive value, systems subject to strong optimization pressures—whether evolutionary (biology) or engineering (protocol design)—exhibit a striking convergence to a narrow range. We identify $a \in [2, 3]$ as the *Thermodynamic Efficiency Frontier* for molecular and information-processing machines that use standard chemical fuels (ATP) and operate at typical biophysical efficiencies (see Appendix B for empirical characterization).

The clustering of the rate parameter in this range reflects a fundamental finite-time thermodynamic tradeoff. Systems with $a < 2$ are noise-dominated, where thermal fluctuations spontaneously reverse error correction, leading to instability. Conversely, systems with $a \gg 3$ approach the reversible limit (“frozen” regime), achieving high accuracy but at vanishingly slow operation speeds. The interval $a \in [2, 3]$ represents the maximum-power regime—the optimal compromise between thermodynamic stability and operational speed.

The Conditional Prediction. The theory does not assert that all systems must have $a \in [2, 3]$. A system with very strong coupling (large η_{cpl} or W_{budget}) could exhibit $a \gg 3$, but such systems typically approach the reversible limit and operate slowly. Conversely, a system with weak coupling could exhibit $a < 2$, but would be noise-dominated and unstable. Instead, the theory makes a *falsifiable conditional prediction*: Given a system that has been optimized for throughput and reliability to operate near this efficiency frontier ($a \in [2, 3]$), its optimal maintenance allocation κ^* is constrained to the 30–50% band.

The observation that *E. coli* kinetic proofreading ($\kappa_{\text{obs}} \approx 0.37$), TCP bulk transfer ($\kappa_{\text{obs}} \approx 0.35$), and non-enzymatic DNA ligation Aoyanagi et al. [2025] all independently occupy the same maintenance band suggests that $\kappa \in [0.30, 0.50]$ is a robust optimum across disparate optimization landscapes. In molecular systems, this is consistent with operation near the thermodynamic efficiency frontier ($a \in [2, 3]$); in TCP, it arises primarily from distributed stability constraints (see Section 6).

Physical Interpretation of a . Biological systems. At $T = 310$ K, ATP/GTP hydrolysis provides $\Delta\mu \sim 20 k_B T$ per molecule. Kinetic proofreading expends 2–4 molecules per discrimination step Hopfield [1974], Johansson et al. [2012], but only a fraction η_{cpl} of this energy couples to the discrimination bias (see Appendix B for the normalization). For well-adapted systems, the effective rate parameter $a \approx 2\text{--}3$ reflects this coupling efficiency.

Network protocols. For ARQ-based systems, the effective rate parameter $a = n_{\text{max}} \ln(1/p)$ where p is the packet loss probability and n_{max} is the maximum permitted transmissions including the initial attempt (see Section 6). For typical parameters ($p \approx 0.01$, $n_{\text{max}} \approx 5$), this yields $a \approx 23$ —larger than the biological range. However, the observed $\kappa_{\text{obs}} \approx 0.30\text{--}0.40$ in bulk TCP is dominated by stability margin and congestion control, not merely ARQ redundancy; the convergence to the

preservation band reflects distributed stability constraints rather than the $a \in [2, 3]$ frontier. The preservation band is a mathematical consequence of the allocation objective $(1 - \kappa)R(\kappa)$ (or, when a nonzero baseline exists, its normalized incremental form $(1 - \kappa)\tilde{R}(\kappa)$; see Section 6) combined with diminishing returns. The physical mechanisms generating these diminishing returns differ across substrates—thermodynamic dissipation in molecular systems, feedback stability in network protocols—but the optimal allocation constraint does not.

Information-theoretic systems. For binary symmetric channels with crossover probability $p = 0.01$, the capacity is $C \approx 0.92$ bits. Achieving error probability 10^{-6} requires blocklength $n \approx 500$, giving effective $a \approx 3\text{--}4$ when normalized appropriately Polyanskiy et al. [2010].

4 The Diminishing-Returns Regime

Having established the physical basis for the exponential-saturation form, we formalize it as a regime definition.

Definition 1 (Diminishing-Returns Regime). *A system operates in the diminishing-returns regime if its reliability function takes the form $R(\kappa) = 1 - e^{-g(\kappa)}$ where $g(0) = 0$, $g'(\kappa) > 0$, and g is concave ($g'' \leq 0$).*

Definition 2 (Smooth Saturation). *A system in the diminishing-returns regime exhibits smooth saturation if, additionally, the rate of error suppression $g'(\kappa)$ varies by at most a factor M over $\kappa \in [0, 1/2]$:*

$$\frac{g'(0)}{g'(1/2)} \leq M \quad (12)$$

for some moderate constant M (e.g., $M \leq 3$). Equivalently, smooth saturation excludes systems with abrupt early saturation where $g'(\kappa)$ drops precipitously after an initial steep region.

The linear reference case $g(\kappa) = a\kappa$ (constant g') satisfies smooth saturation with $M = 1$. Empirically, systems with $a \in [2, 3]$ and smooth saturation typically exhibit κ^* in the 30–50% band;

the lower bound arises because moderate a values prevent the stiffness from growing too rapidly at small κ .

The concavity of $g(\kappa)$ corresponds to diminishing marginal returns in error suppression: each additional unit of maintenance investment yields a smaller reduction in error probability. As shown in Section 3, this behavior emerges from fundamental constraints—finite channel capacity and bounded dissipation budgets—rather than model-specific assumptions.

Empirically, diminishing returns are observed in kinetic proofreading Hopfield [1974], classical coding below threshold Gallager [1965], and fault-tolerant computing. Systems exhibiting sharp threshold effects (e.g., LDPC codes near capacity Richardson and Urbanke [2001]) have convex g and are explicitly excluded from the present framework. Such systems undergo phase transitions and require separate treatment.

For reliability functions of the exponential-saturation form, the stiffness has an explicit expression:

$$\mathcal{S}_\kappa = \frac{e^{g(\kappa)} - 1}{\kappa g'(\kappa)}. \quad (13)$$

For the reference case $g(\kappa) = a\kappa$ (constant error suppression rate), this simplifies to

$$\mathcal{S}_\kappa = \frac{e^{a\kappa} - 1}{a\kappa}. \quad (14)$$

This is the formula used to generate the curves in Fig. 1.

5 The Preservation Band

For systems in the diminishing-returns regime, the stiffness is bounded below, which constrains the optimal maintenance fraction.

Theorem 1 (Upper Bound). *For any reliability function $R(\kappa) = 1 - e^{-g(\kappa)}$ with $g(0) = 0$, $g'(\kappa) > 0$ for $\kappa > 0$, and g concave ($g'' \leq 0$), we have $\mathcal{S}_\kappa > 1$ for all $\kappa > 0$, with $\lim_{\kappa \rightarrow 0^+} \mathcal{S}_\kappa = 1$.*

Proof. See Appendix A for a detailed derivation. The key step is showing that $R''(\kappa) = (g'' - (g')^2)e^{-g} < 0$ for $\kappa > 0$, which holds because $g'' \leq 0$ and $(g')^2 > 0$. This implies $R(\kappa) > \kappa R'(\kappa)$ and hence $\mathcal{S}_\kappa > 1$. \square

Since $\mathcal{S}_\kappa > 1$ for all $\kappa > 0$ (Theorem 1), and the optimal κ^* is interior, the Stiffness-Odds Identity (Eq. 3) gives

$$\frac{1 - \kappa^*}{\kappa^*} = \mathcal{S}_\kappa(\kappa^*) > 1 \implies \kappa^* < \frac{1}{2}. \quad (15)$$

The upper bound $\kappa^* < 0.50$ is unconditional for any system in the diminishing-returns regime. It follows from the concavity of g and positivity of g' (which together imply $\mathcal{S}_\kappa > 1$), without assumptions about the rate parameter. Conversely, empirical observation of $\mathcal{S}_\kappa \leq 1$ is diagnostic evidence that a system operates outside this regime—signaling threshold effects, cooperative dynamics, or correlated failures.

Lower Bound (Conditional). The rate parameter $a = g'(0)$ characterizes the initial steepness of error suppression. For the reference case $g(\kappa) = a\kappa$, the stiffness at $\kappa = 1/2$ is

$$c(a) = \mathcal{S}_\kappa(1/2) = \frac{e^{a/2} - 1}{a/2}. \quad (16)$$

The Stiffness-Odds Identity then gives the lower bound $\kappa^* \geq 1/(1 + c(a))$.

Since $c(a)$ is increasing in a , **larger rate parameters push the lower bound down**: more efficient error suppression allows systems to achieve target reliability with less maintenance. **The lower bound $\kappa^* \geq 0.30$ holds for $a \leq 3$** , which characterizes systems operating near the thermodynamic efficiency frontier (Section 3). Systems with $a < 2$ —requiring greater maintenance investment per unit of error suppression—would optimize at *higher* κ^* , potentially exceeding 0.37. Systems with $a > 3$ exhibit strong coupling but slow kinetics (approaching the reversible limit); the lower bound drops below 0.30, but such systems are rare among those under selection pressure for throughput.

The 30–50% band is therefore a prediction for physically realistic systems operating near the efficiency frontier with $a \in [2, 3]$, not a mathematical necessity for all diminishing-returns systems.

For more general concave g , the lower bound depends on the specific curvature; the linear

case provides a reference estimate for systems with approximately constant error-suppression rate. Systems with abrupt early saturation—where $g'(\kappa)$ drops rapidly after an initial steep region—may optimize at lower κ^* , though such behavior is not observed in the empirical examples considered here. For $a \in [2, 3]$, we have $c(a) \in [1.7, 2.3]$ and hence $\kappa^* \in [0.30, 0.50]$ for systems with smooth saturation.

6 Validation and Scope

The theoretical band $\kappa^* \in [0.3, 0.5]$ serves as a diagnostic tool for systems in the diminishing-returns regime.

Biological Proofreading. In *E. coli* protein synthesis, kinetic proofreading consumes GTP to discriminate between correct and incorrect codon matches. The energetic cost is approximately $3\text{--}4 k_B T$ per peptide bond to achieve an error rate of 10^{-4} Hopfield [1974]. Based on measurements of GTP consumption during translation Johansson et al. [2012], Loveland et al. [2017], the maintenance fraction—defined as the ratio of proofreading energy expenditure to translation-specific energy budget (EF-Tu and EF-G mediated GTP hydrolysis, excluding upstream aminoacylation costs independent of the fidelity mechanism)—is estimated at $\kappa_{\text{obs}} \approx 0.35\text{--}0.40$. This sits squarely within the predicted interior band, suggesting that biological error correction operates near the thermodynamic efficiency frontier defined by Eq. (3). Recent experiments in non-enzymatic DNA ligation confirm that this kinetic proofreading mechanism is not limited to evolved enzymes, but arises as a fundamental thermodynamic property of information replication in synthetic systems Aoyanagi et al. [2025].

Network Reliability Protocols. TCP/IP provides a non-biological example where preservation overhead is both engineered and well documented. The protocol stack maintains end-to-end reliability through checksums, sequence numbers, acknowledgments, retransmis-

sions, and congestion control—all of which consume channel capacity that would otherwise carry payload.

We define the maintenance fraction as the fraction of channel capacity not delivered as payload (goodput). For TCP, κ should be interpreted as the fraction of link capacity diverted from payload either into explicit protocol overhead (headers, ACKs, retransmissions) *or* into stability margin (deliberate under-utilization required for congestion stability). This κ is therefore a control/response variable of a distributed feedback system, not a purely local energetic cost as in molecular proofreading.

Empirical studies of TCP congestion control report that, under typical Internet path conditions (packet loss rates on the order of $10^{-3}\text{--}10^{-2}$ and moderate congestion), goodput efficiencies of 60–70% are common for long-lived flows, corresponding to $\kappa_{\text{obs}} \approx 0.30\text{--}0.40$ Mathis et al. [1997], Ha et al. [2008]. This overhead arises from protocol headers, acknowledgment traffic, retransmissions, and—most significantly—capacity left unused by loss-based congestion control algorithms that reduce sending rates in response to packet loss.

Note on TCP quantification: The TCP estimate is qualitative, derived from typical goodput efficiencies under congestion; systematic measurement of the reliability function $R(\kappa)$ for specific TCP variants—varying retransmission limits, congestion windows, and loss rates to trace out the full curve—remains an empirical opportunity. The $\kappa_{\text{obs}} \approx 0.35$ figure should be understood as an order-of-magnitude estimate consistent with the framework, not a precise measurement of the kind available for biological proofreading.

As a stylized model, consider independent packet losses with probability p , and permit up to n total transmissions. We restrict attention to the *link-error dominated regime* where p reflects exogenous channel impairments (random bit errors, fading) rather than endogenous congestion—an approximation valid for low-utilization or wireless links but not for congestion-controlled flows where p depends on the control algorithm itself. Under this restric-

tion, the probability that a message is delivered correctly within a timeout window is

$$R(n) \approx 1 - p^n. \quad (17)$$

In the stylized ARQ-only model below, κ denotes the *redundancy component* of total TCP overhead; in real TCP, the observed κ_{obs} additionally includes stability margin from congestion control.

To map this to our framework, we define $\kappa(n) := (n - 1)/n_{\text{max}}$, where n_{max} is the maximum permitted transmissions including the initial attempt (a protocol parameter). This gives $\kappa \in [0, 1]$ with $\kappa = 0$ corresponding to no redundancy ($n = 1$). Substituting yields

$$R(n) = 1 - p^{1+\kappa n_{\text{max}}} = 1 - p \cdot e^{-\kappa n_{\text{max}} \ln(1/p)}. \quad (18)$$

Reconciling with the framework. Note that $R(0) = 1 - p \neq 0$, whereas our formal regime definition requires $R(0) = 0$ (from $g(0) = 0$). To apply the framework, we define the *normalized reliability improvement*:

$$\tilde{R}(\kappa) := \frac{R(\kappa) - R_0}{1 - R_0}, \quad R_0 := R(0) = 1 - p. \quad (19)$$

This gives $\tilde{R}(0) = 0$ and $\tilde{R}(\kappa) = 1 - e^{-a\kappa}$ with $a = n_{\text{max}} \ln(1/p)$, which is exactly the exponential-saturation form. For typical parameters ($p \approx 0.01$, $n_{\text{max}} \approx 5$), this yields $a \approx 23$ —larger than the biological range. Under this normalization, Eq. (3) applies to the incremental-throughput objective $(1 - \kappa)\tilde{R}(\kappa)$; we therefore compute $\tilde{\mathcal{S}}_\kappa := \tilde{R}/(\kappa\tilde{R}')$ —the stiffness of the incremental reliability improvement—and compare it to the resource-odds condition.

Crucially, this standard ARQ model is mathematically isomorphic to the linear reference ansatz $g(\kappa) = a\kappa$ used in Fig. 1, with the effective rate parameter $a \propto -\ln p$ determined by the channel noise. For such models, and for throughput-reliability curves reported for high-speed TCP variants Ha et al. [2008], typical operating points correspond to normalized stiffnesses $\tilde{\mathcal{S}}_\kappa$ of order 1–2, consistent with the equilibrium condition of Eq. (3).

Unlike biological systems shaped by evolution, network protocols are engineered artifacts. That

both classes of systems converge to similar maintenance fractions supports the interpretation of the preservation band as a structural constraint, rather than a historical accident. This convergence is particularly striking because TCP designers optimized for throughput under real-world conditions without knowledge of kinetic proofreading or thermodynamic bounds on error correction—yet arrived at overhead ratios indistinguishable from those selected by 3.5 billion years of biological evolution. Moreover, the band appears to function as an attractor in design space: protocols that attempt to operate below $\kappa \approx 0.30$ (aggressive transmission with minimal acknowledgment) suffer stability failures under congestion, while those exceeding $\kappa \approx 0.50$ (excessive redundancy and conservative rate control) systematically underutilize available capacity. The observed convergence thus reflects not engineering convention but the shape of the underlying optimization landscape.

Scope and Limitations. The diminishing-returns assumption holds for memoryless noise channels with independent errors and for systems operating below coding thresholds. In systems dominated by burst errors, long-range correlations, or cooperative failure mechanisms, $R(\kappa)$ may exhibit convex regions or sharp thresholds. This breakdown is analogous to the waterfall region in LDPC decoding, where reliability exhibits a sharp transition rather than smooth saturation Richardson and Urbanke [2001]. In these regimes, the interior band solution is replaced by corner solutions (all-or-nothing protection), and the present framework does not apply.

The preservation band should therefore be understood as characterizing the “smooth reliability regime” where error suppression saturates gradually. The empirical success of the prediction for both kinetic proofreading and network protocols suggests this regime is physically significant.

6.1 The Stiffness as a Diagnostic

Figure 2 recasts Eq. (3) as a phase diagram in the $(\kappa, \mathcal{S}_\kappa)$ plane (for systems with nonzero base-

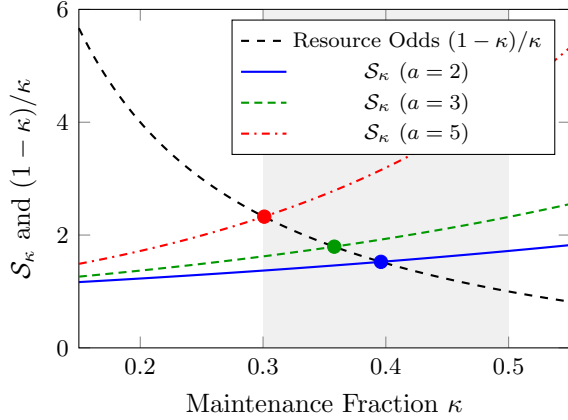


Figure 1: Equilibrium condition for preservation in the diminishing-returns regime. The dashed black curve shows the resource odds $(1 - \kappa)/\kappa$. Colored curves show the preservation stiffness $S_\kappa = (e^{a\kappa} - 1)/(a\kappa)$ for rate parameters $a = 2, 3, 5$ (Eq. 14). Intersections (dots) define the optimal maintenance fraction κ^* . The gray band marks the predicted 30–50% regime. For $a = 3$ (typical of biological proofreading), the intersection occurs at $\kappa^* \approx 0.36$.

line reliability such as TCP, the normalized stiffness \tilde{S}_κ is used; see Section 6). The dashed curve $S_\kappa = (1 - \kappa)/\kappa$ is the equilibrium locus at which stiffness matches the resource odds. Points above this curve correspond to a “stiff” mode, where error suppression is saturated and maintenance is over-allocated; points below correspond to a “soft” mode, where reliability remains highly responsive to additional maintenance. The diagram makes S_κ a practical diagnostic: given an empirical estimate of (κ, S_κ) , one can immediately read off whether a system under- or over-invests in maintenance.

6.2 Falsifiability

The preservation band is a conditional prediction: *given* that a system operates in the diminishing-returns regime, *then* its optimal maintenance fraction lies in the interior range $\kappa^* \in [0.30, 0.50]$ and its stiffness satisfies $S_\kappa > 1$ at the operating point.

The protocol is substrate-agnostic: the same measurements of $R(\kappa)$, κ_{obs} , and S_κ apply

whether maintenance is implemented via GTP hydrolysis in biology, protocol overhead in communication networks, or parity bits and redundancy in digital storage.

This prediction can be tested empirically via the following protocol:

- 1. Confirm regime membership.** Measure the reliability function $R(\kappa)$ across the accessible range of maintenance investment. Compute $g(\kappa) = -\ln(1 - R(\kappa))$ and verify that g is concave ($g'' \leq 0$), confirming diminishing returns. Systems that exhibit sharp threshold behavior—for example, abrupt changes in $R(\kappa)$ at a critical κ —lie outside the present framework and cannot falsify it.
- 2. Measure the operating point.** Determine the system’s actual maintenance fraction κ_{obs} and reliability R_{obs} . In biological systems, this requires calorimetric or stoichiometric estimates of resources devoted to error correction versus payload production. In engineered systems, protocol overhead and capacity accounting usually suffice.
- 3. Compute the stiffness.** From the measured $R(\kappa)$ curve, evaluate $S_\kappa = R/(\kappa R')$ at κ_{obs} , either by differentiating a parametric fit or by finite differences on the empirical data.
- 4. Test the predictions.** A system that satisfies the concavity condition in step 1 but exhibits $\kappa^* > 0.50$, or $S_\kappa < 1$ at its operating point, would directly falsify the preservation band.

It is important to distinguish falsification from scope exclusion. A system displaying $S_\kappa < 1$ may simply operate outside the diminishing-returns regime, for instance due to cooperative failures, threshold coding, or long-range correlations in the noise. Such observations do not falsify the theory; rather, they confirm the diagnostic power of S_κ in identifying regime boundaries. Falsification requires a system that demonstrably satisfies the diminishing-returns condition (concave g) yet violates the predicted bounds on κ^* or S_κ .

Promising candidates for stringent tests include: (i) redundant storage arrays (RAID),

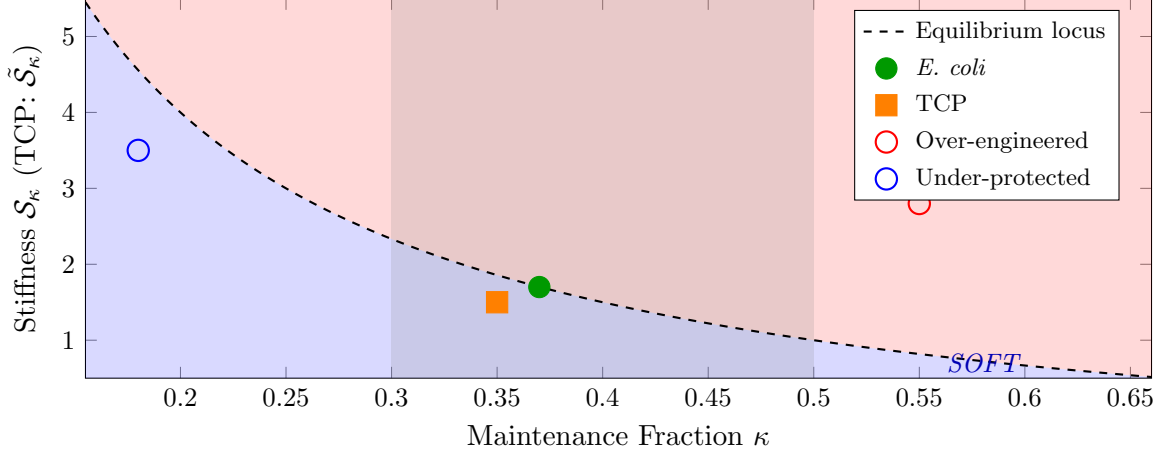


Figure 2: Preservation phase diagram in the (κ, S_κ) plane. The dashed curve shows the resource-odds relation $S_\kappa = (1 - \kappa)/\kappa$ (Eq. 3), which forms the equilibrium locus where stiffness matches the leverage of maintenance resources. The region above the curve (shaded red) corresponds to a stiff mode, $S_\kappa > (1 - \kappa)/\kappa$, in which error suppression is saturated and additional maintenance yields small reliability gains relative to the payload capacity sacrificed. The region below (shaded blue) corresponds to a soft mode, $S_\kappa < (1 - \kappa)/\kappa$, where the system is under-protected and additional maintenance would improve effective throughput. A gray vertical band marks the predicted maintenance range $\kappa \in [0.30, 0.50]$ for systems in the diminishing-returns regime. Markers indicate illustrative operating points: empirical κ estimates paired with stiffness values computed from the linear reference model (Eq. 14). *E. coli* kinetic proofreading ($\kappa \approx 0.37$, $S_\kappa \sim 1.7$) and TCP bulk transfer ($\kappa \approx 0.35$, $\tilde{S}_\kappa \sim 1.5$; normalized stiffness, see Section 6) both lie near the equilibrium locus; hypothetical over-engineered and under-protected configurations are shown for comparison.

where redundancy level and capacity overhead are tunable and reliability curves are well characterized; (ii) ribosomal proofreading across species, where organisms with different metabolic constraints may optimize at different points along the band; and (iii) software fault-tolerance schemes such as N -version programming and recovery blocks in safety-critical systems, where the objective function effectively corresponds to $\alpha > 1$ in the notation of Sec. 7. The framework thus predicts not only typical maintenance fractions, but also its own boundaries: values $S_\kappa < 1$ serve as a diagnostic of regimes where preservation is governed by threshold phenomena and phase-transition physics rather than smooth response theory.

7 Robustness and the Asymmetry of Risk

Our analysis thus far has identified the optimal maintenance fraction κ^* by locating the peak of the effective throughput. However, biological and engineered systems rarely operate exactly at a mathematical peak. A critical question is the *stability* of this operating point: what are the consequences of deviating from κ^* ?

We examine the “landscape of risk” by analyzing the shape of the throughput curve $T_{\text{eff}}(\kappa)$. As shown in Figure 3, the penalty for deviation is fundamentally asymmetric.

The Error Cliff vs. The Stagnation Slope. To the left of the band ($\kappa < 0.30$), the system is dominated by the exponential term in the reliability function $R(\kappa) = 1 - e^{-g(\kappa)}$. A small reduction in maintenance leads to a catastrophic rise

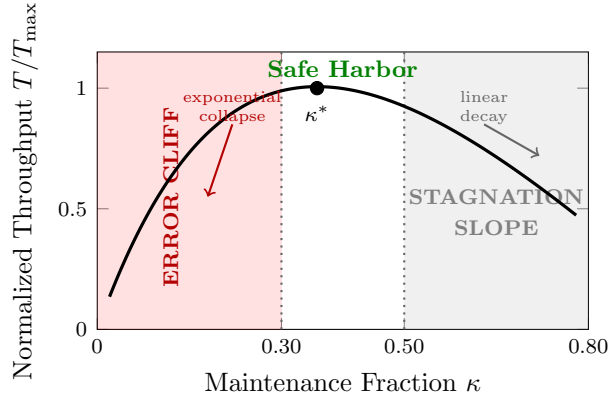


Figure 3: The Stability Landscape ($a = 3$). The penalty for deviating from the optimal maintenance band is asymmetric. To the left ($\kappa < 0.30$), systems face an “Error Cliff” where reliability collapses exponentially, leading to catastrophic failure. To the right ($\kappa > 0.50$), systems enter a “Stagnation Slope” where throughput decays only linearly due to capacity waste. This asymmetry creates strong selection pressure favoring the preservation band as a “safe harbor,” trapping optimized systems in the 30–50% regime.

in error probability, causing effective throughput to collapse. We term this region the **Error Cliff**.

To the right of the band ($\kappa > 0.50$), reliability saturates ($R \approx 1$). Further investment yields negligible error reduction, and the throughput decay is dominated by the linear term $(1 - \kappa)$. We term this region the **Stagnation Slope**.

Evolutionary and Engineering Implications. This topological asymmetry resolves why systems as diverse as bacterial ribosomes and network protocols converge to the same maintenance window. They are not merely seeking a peak; they are *avoiding a cliff*.

Evolutionary or engineering gradients driving a system from minimal maintenance ($\kappa \approx 0$) experience strong negative feedback (death/failure), rapidly pushing the system up the cliff. Once the system crests into the 30–50% band, the gradient flattens dramatically. The penalty for overshooting into the Stagnation Slope is mild (inefficiency) compared to the

penalty for undershooting (instability). Robust systems therefore “accumulate” in this band, trapped by the asymmetry of thermodynamic risk.

This explains why the preservation band functions as a broad basin of attraction rather than a knife-edge optimum. Systems need not be precisely tuned; they need only avoid the cliff. The empirical clustering observed in biology and technology reflects this asymmetric selection pressure.

Robustness to Objective Variation. The results above assume systems maximize effective throughput $T_{\text{eff}} = (1 - \kappa)R(\kappa)$. Systems that weight reliability more heavily might maximize $(1 - \kappa)R(\kappa)^\alpha$ for $\alpha > 1$. The first-order condition yields $S_\kappa(\kappa^*) = \alpha(1 - \kappa^*)/\kappa^*$, shifting κ^* upward as α increases. The band widens but persists: the upper bound becomes $\kappa^* \leq \alpha/(1 + \alpha)$, approaching unity only as $\alpha \rightarrow \infty$.

8 Multi-Dimensional Extension

The scalar analysis extends to systems with multiple maintenance channels. For vector allocation $\boldsymbol{\kappa} = (\kappa_1, \dots, \kappa_m)$ with total maintenance $\kappa_{\text{tot}} = \sum_i \kappa_i$, suppose the reliability function factorizes or admits a sufficient statistic in κ_{tot} : $R(\boldsymbol{\kappa}) = R(\kappa_{\text{tot}})$.

The first-order conditions for maximizing $(1 - \kappa_{\text{tot}})R(\kappa_{\text{tot}})$ yield the same Stiffness-Odds Identity with κ_{tot} replacing κ :

$$S_{\kappa_{\text{tot}}}(\kappa_{\text{tot}}^*) = \frac{1 - \kappa_{\text{tot}}^*}{\kappa_{\text{tot}}^*}. \quad (20)$$

The band $[0.30, 0.50]$ therefore applies to *total* maintenance allocation regardless of its decomposition across channels. The internal allocation among κ_i depends on the marginal reliabilities $\partial R / \partial \kappa_i$, but the aggregate constraint persists. This result is relevant for systems where maintenance takes multiple forms (e.g., temporal redundancy, spatial redundancy, and active error correction in fault-tolerant computing).

9 Conclusion

We have characterized preservation as a distinct operational regime within the diminishing-returns class, governed by the stiffness \mathcal{S}_κ . In biochemical systems this regime is constrained by dissipation; in engineered protocols it is constrained by stability margins—but the allocation geometry is shared. The Stiffness-Odds Identity provides a physical explanation for the maintenance overheads observed in robust systems operating in this regime: bounded above by 50% in general, and concentrated in the 30–50% band for systems with smooth saturation—a pattern observed from cellular biology and synthetic chemistry to fault-tolerant computing and network protocols. Preservation is not merely about minimizing error; it is about matching the stiffness of the repair mechanism to the leverage of available resources.

The dual physical derivation (Section 3) establishes that the diminishing-returns regime is not an assumption but a consequence of fundamental constraints: Shannon’s channel capacity bounds the information-theoretic route, while Landauer’s erasure principle bounds the thermodynamic route. Their convergence on the same exponential-saturation form is the paper’s central theoretical contribution, grounding the preservation band in physics rather than phenomenology. The convergence of biochemical (*E. coli*) and engineered (TCP/IP) systems to the same maintenance band supports the interpretation that the preservation constraint is structural—a property of the optimization landscape under diminishing returns—rather than tied to a single substrate-specific mechanism.

The framework explicitly excludes systems near coding thresholds or with cooperative error mechanisms, where reliability exhibits sharp transitions. Characterizing such systems remains an open problem, likely requiring tools from the statistical mechanics of phase transitions.

The preservation stiffness framework may extend to external oversight of complex systems. In forthcoming work Brandes [forthcoming], we explore whether human oversight of AI decisions

faces an analogous bandwidth constraint; the connection remains conjectural but suggestive.

The diagnostic power of \mathcal{S}_κ extends beyond prediction to system design: measuring a system’s position in the $(\kappa, \mathcal{S}_\kappa)$ plane immediately reveals whether it under- or over-invests in maintenance, providing actionable guidance for optimization.

A Derivation of the Stiffness Bound

We prove Theorem 1: for any reliability function $R(\kappa) = 1 - e^{-g(\kappa)}$ with $g(0) = 0$, $g'(\kappa) > 0$, and g concave, the preservation stiffness satisfies $\mathcal{S}_\kappa > 1$ for all $\kappa > 0$.

Lemma 1. *Define $\varphi(\kappa) = R(\kappa) - \kappa R'(\kappa)$. For $R(\kappa) = 1 - e^{-g(\kappa)}$ with g concave and $g(0) = 0$, we have $\varphi(\kappa) > 0$ for all $\kappa > 0$.*

Proof. We proceed by analyzing φ at the boundary and in the interior.

Step 1: Boundary behavior. At $\kappa = 0$:

$$R(0) = 1 - e^{-g(0)} = 1 - e^0 = 0, \quad (21)$$

$$R'(\kappa) = g'(\kappa)e^{-g(\kappa)}, \quad (22)$$

$$R'(0) = g'(0)e^0 = g'(0) > 0. \quad (23)$$

Thus $\varphi(0) = R(0) - 0 \cdot R'(0) = 0$.

Step 2: Derivative of φ . We compute:

$$\varphi'(\kappa) = R'(\kappa) - R'(\kappa) - \kappa R''(\kappa) = -\kappa R''(\kappa). \quad (24)$$

Step 3: Sign of R'' . For $R(\kappa) = 1 - e^{-g(\kappa)}$:

$$R' = g'e^{-g}, \quad (25)$$

$$R'' = g''e^{-g} - (g')^2e^{-g} = (g'' - (g')^2)e^{-g}. \quad (26)$$

Since $g'' \leq 0$ (concavity) and $(g')^2 > 0$, we have $g'' - (g')^2 < 0$, hence $R'' < 0$ for all $\kappa > 0$.

Step 4: Positivity of φ . Since $R'' < 0$, we have $\varphi'(\kappa) = -\kappa R''(\kappa) > 0$ for $\kappa > 0$. Combined with $\varphi(0) = 0$, this implies $\varphi(\kappa) > 0$ for all $\kappa > 0$. \square

Proof of Theorem 1. From Lemma 1, $R(\kappa) - \kappa R'(\kappa) > 0$ for $\kappa > 0$. Since $R(\kappa) > 0$ and

$R'(\kappa) > 0$ for $\kappa > 0$ (as $R(\kappa) = 1 - e^{-g(\kappa)}$ with $g' > 0$), we can divide:

$$\frac{R(\kappa) - \kappa R'(\kappa)}{R(\kappa)} > 0 \implies 1 - \frac{\kappa R'(\kappa)}{R(\kappa)} > 0. \quad (27)$$

Rearranging:

$$\frac{R(\kappa)}{\kappa R'(\kappa)} > 1 \implies \mathcal{S}_\kappa > 1. \quad (28)$$

□

Remark. The proof relies only on the concavity of g ($g'' \leq 0$), positivity of g' , and the boundary condition $g(0) = 0$. No assumption about the rate parameter $a = g'(0)$ is required. The strict bound $\mathcal{S}_\kappa > 1$ holds for all $\kappa > 0$. In the limit $\kappa \rightarrow 0^+$, L'Hôpital's rule gives $\mathcal{S}_\kappa \rightarrow 1$, confirming the theorem statement.

B Thermodynamic Bound on the Rate Parameter

We characterize the range $a \in [2, 3]$ as the *Thermodynamic Efficiency Frontier*—the empirical cluster of systems that have been optimized (by evolution or engineering) to efficiently couple maintenance resources to error suppression.

Clarification on epistemology. The bound $a \in [2, 3]$ is not derived from first principles as a universal constant. Rather, it represents an empirical characterization of the parameter range occupied by well-adapted systems operating at finite speed. The theory's prediction is conditional: *if* a system operates near this efficiency frontier, *then* its optimal κ^* falls in the 30–50% band. Systems with very large a (strong coupling, approaching the reversible limit with slow kinetics) or very small a (weak coupling, noise-dominated) are physically possible but atypical among systems under selection pressure for throughput.

Normalization and bookkeeping. To avoid ambiguity, we distinguish extensive and intensive quantities explicitly:

Let $\Delta\mu$ denote the chemical free energy available per ATP/GTP hydrolysis ($\Delta\mu \approx 20 k_B T$).

Let n_{ATP} be the mean number of hydrolyses expended per discrimination event (including futile cycles). The total dissipated work per discrimination is then $W_{\text{diss}} = n_{\text{ATP}} \Delta\mu$ —an *extensive* cost.

We parameterize maintenance investment by the dimensionless fraction $\kappa := W_{\text{diss}}/W_{\text{budget}}$, where W_{budget} is the total resource budget per decision (payload + maintenance) in the same units. Under this normalization, *increasing* n_{ATP} *increases* κ (higher maintenance share), rather than changing the coupling strength a .

Only a fraction $\eta_{\text{cpl}} \in (0, 1)$ of W_{diss} contributes to biasing the correct outcome; hence the suppression exponent satisfies

$$g(\kappa) \equiv -\ln(1 - R(\kappa)) \approx \eta_{\text{cpl}} \frac{W_{\text{diss}}}{k_B T} = \eta_{\text{cpl}} \frac{W_{\text{budget}}}{k_B T} \kappa \quad (29)$$

in the smooth regime. Therefore the rate parameter is

$$a = g'(0) = \eta_{\text{cpl}} \frac{W_{\text{budget}}}{k_B T}. \quad (30)$$

Physical interpretation. Under this normalization:

- The rate parameter a is an *intensive* coupling strength: higher η_{cpl} (better energy-to-discrimination conversion) yields larger a .
- The maintenance fraction κ is an *extensive* cost: more futile cycles increase κ at fixed W_{budget} , but do not directly change a .
- Any degradation due to futile cycling enters through the empirical κ accounting (and potentially through reduced η_{cpl} if cycles are reliability-neutral), not through an explicit $1/n_{\text{ATP}}$ factor in a .

Empirical characterization of the frontier. For ATP-driven molecular machines at physiological conditions ($W_{\text{budget}} \sim 40\text{--}60 k_B T$ per decision, accounting for both payload synthesis and proofreading), observed coupling efficiencies $\eta_{\text{cpl}} \in [0.04, 0.08]$ yield $a \in [2, 4]$. Well-adapted systems cluster near $a \approx 2.5\text{--}3$, corresponding to the regime where discrimination energy ($\sim 2\text{--}3 k_B T$ per unit κ) exceeds thermal noise but does not approach the reversible limit.

Interpretation of bounds. Lower bound ($a \geq 2$): Systems with $a < 2$ are weakly coupled (small effective discrimination energy per unit κ). Achieving a target reliability therefore requires a larger maintenance fraction, making such systems throughput-disfavored. The discrimination barrier would be less than $2k_B T$, making error correction susceptible to spontaneous reversal by thermal fluctuations.

Upper bound ($a \leq 3$ for optimized systems): Systems with $a > 3$ achieve high coupling strength but typically at the cost of slow operation (approaching the reversible limit). Such systems are rare among those under selection pressure for throughput.

Summary. The preservation band $\kappa^* \in [0.30, 0.50]$ is robust for the specific (but broad) class of ATP-fueled and analogously efficient systems that have optimized their energetic coupling to settle in the $a \in [2, 3]$ regime. Biological proofreading and synthetic chemistry converge to this band via the thermodynamic efficiency frontier. Network protocols converge to similar κ values through a different mechanism—distributed stability constraints that penalize both under-protection (instability) and over-protection (under-utilization)—demonstrating that the preservation band emerges from multiple independent optimization pressures.

References

C. E. Shannon. A mathematical theory of communication. *Bell Syst. Tech. J.*, 27:379–423, 1948.

R. Landauer. Irreversibility and heat generation in the computing process. *IBM J. Res. Dev.*, 5:183–191, 1961.

J. J. Hopfield. Kinetic proofreading: A new mechanism for reducing errors in biosynthetic processes requiring high specificity. *Proc. Natl. Acad. Sci. U.S.A.*, 71:4135–4139, 1974.

R. G. Gallager. A simple derivation of the coding theorem and some applications. *IEEE Trans. Inf. Theory*, 11:3–18, 1965.

Y. Polyanskiy, H. V. Poor, and S. Verdú. Channel coding rate in the finite blocklength regime. *IEEE Trans. Inf. Theory*, 56:2307–2359, 2010.

U. Seifert. Stochastic thermodynamics, fluctuation theorems and molecular machines. *Rep. Prog. Phys.*, 75:126001, 2012.

J. M. R. Parrondo, J. M. Horowitz, and T. Sagawa. Thermodynamics of information. *Nat. Phys.*, 11:131–139, 2015.

G. E. Crooks. Entropy production fluctuation theorem and the nonequilibrium work relation for free energy differences. *Phys. Rev. E*, 60:2721–2726, 1999.

T. J. Richardson and R. L. Urbanke. The capacity of low-density parity-check codes under message-passing decoding. *IEEE Trans. Inf. Theory*, 47:599–618, 2001.

M. Johansson, J. Zhang, and M. Ehrenberg. Genetic code translation displays a linear trade-off between efficiency and accuracy of tRNA selection. *Proc. Natl. Acad. Sci. U.S.A.*, 109:131–136, 2012.

A. B. Loveland, G. Demo, N. Grigorieff, and A. A. Korostelev. Ensemble cryo-EM elucidates the mechanism of translation fidelity. *Nature*, 546:113–117, 2017.

H. Aoyanagi, Y. Magi, and S. Toyabe. Experimental demonstration of kinetic proofreading inherited in ligation-based information replication. *Phys. Rev. Research*, 7:043263, 2025.

M. Mathis, J. Semke, J. Mahdavi, and T. Ott. The macroscopic behavior of the TCP congestion avoidance algorithm. *ACM SIGCOMM Comput. Commun. Rev.*, 27(3):67–82, 1997.

S. Ha, I. Rhee, and L. Xu. CUBIC: A new TCP-friendly high-speed TCP variant. *ACM SIGOPS Oper. Syst. Rev.*, 42(5):64–74, 2008.

A. Brandes. The Alignment Bandwidth Theorem: Information-Theoretic Limits on Human Oversight of AI Systems. *Forthcoming*.

B. Qureshi, J. M. Poulton, and T. E. Ouldridge. Thermodynamic limits in far-from-equilibrium molecular templating networks. *Newton*, 2025.